View metadata, citation and similar papers at core.ac.uk

brought to you by CORE

provided by East Tennessee State University

East Tennessee State University
Digital Commons @ East Tennessee State University

Undergraduate Honors Theses | Student Works

5-2017

Effect of Cannabinoids on Osteogenic Differentiation of Cultured Vascular Smooth Muscle Cells

Bree A. Eccles
East Tennessee State University

Follow this and additional works at: https://dc.etsu.edu/honors


Part of the Cardiovascular Diseases Commons

Recommended Citation
Eccles, Bree A., "Effect of Cannabinoids on Osteogenic Differentiation of Cultured Vascular Smooth Muscle Cells" (2017). *Undergraduate Honors Theses.* Paper 392. https://dc.etsu.edu/honors/392

This Honors Thesis - Withheld is brought to you for free and open access by the Student Works at Digital Commons @ East Tennessee State University. It has been accepted for inclusion in Undergraduate Honors Theses by an authorized administrator of Digital Commons @ East Tennessee State University. For more information, please contact digilib@etsu.edu.

Effect of Cannabinoids on Osteogenic Differentiation of Cultured Vascular Smooth Muscle Cells

By

Bree Eccles

An Undergraduate Thesis Submitted in Partial Fulfillment
of the Requirements for the
Honors-in-Discipline Chemistry Program and
Midway Honors Scholars Program
College of Arts and Sciences
East Tennessee State University

Bree Eccles Date

Dr. Douglas P. Thewke, Thesis Mentor Date

Dr. Antonio E. Rusiñol, Reader Date

Dr. Karen Kornweibel, Reader Date

Contents

Introduction

Atherosclerosis

Atherosclerosis is a chronic inflammatory vascular disease characterized by the formation of cholesterol-filled lesions within the arterial wall. The formation of raised, often calcified lesions in the arterial intima leads to narrowing of vessels and blockage of blood flow, reducing arterial compliance [1]. Heart disease, specifically atherosclerosis, is the leading cause of morbidity and mortality on a global scale [2]. A large risk factor for this disease is an increased blood concentration of primarily low-density lipoproteins (LDL), so called “bad cholesterol” [2]. However, this disease often coincides with other risk factors including smoking, hypertension, diabetes mellitus, the male sex, and a genetic history of the disease [2].

The formation of atherosclerotic lesions begins when low-density lipoprotein (LDL) crosses the lining of the endothelium and becomes oxidized to form OX-LDL within the arterial wall [3]. Monocytes are recruited to the area and transform into macrophages that engulf the lipoproteins and form foam cells – the signature of atherosclerosis [3]. Ingestion of oxLDL induces macrophage apoptosis, or programmed cell death. The buildup of cellular debris from apoptosis and other materials in the vessel wall forms the atherosclerotic lesion. Foam cells combine with leukocytes to become a fatty streak, and as the process continues, foam cells secrete pro-inflammatory growth factors that induce smooth muscle cells to migrate into the area [3]. These vascular smooth muscle cells (VSMC) secrete extracellular matrix components to help stabilize the lesion. As the lesion progresses, it may become calcified by mechanisms involving the trans-differentiation of VSMC into osteoblast-like cells, thus

forming a plaque. A plaque is considered stable when the lipid core is covered by a thick SMC-saturated fibrous cap. If the fibrous cap weakens and ruptures, the underlying materials will interact with platelets and coagulation factors and form a thrombosis (a blood clot). The thrombus that forms may dislodge and cause blockage of blood flow. The blockage of blood flow presents serious health risks – the deprivation of oxygen to downstream tissue leads to the clinical manifestations of atherosclerosis, heart attacks and strokes [4]. The formation of an atherosclerotic lesion is demonstrated in Figure 1 below:

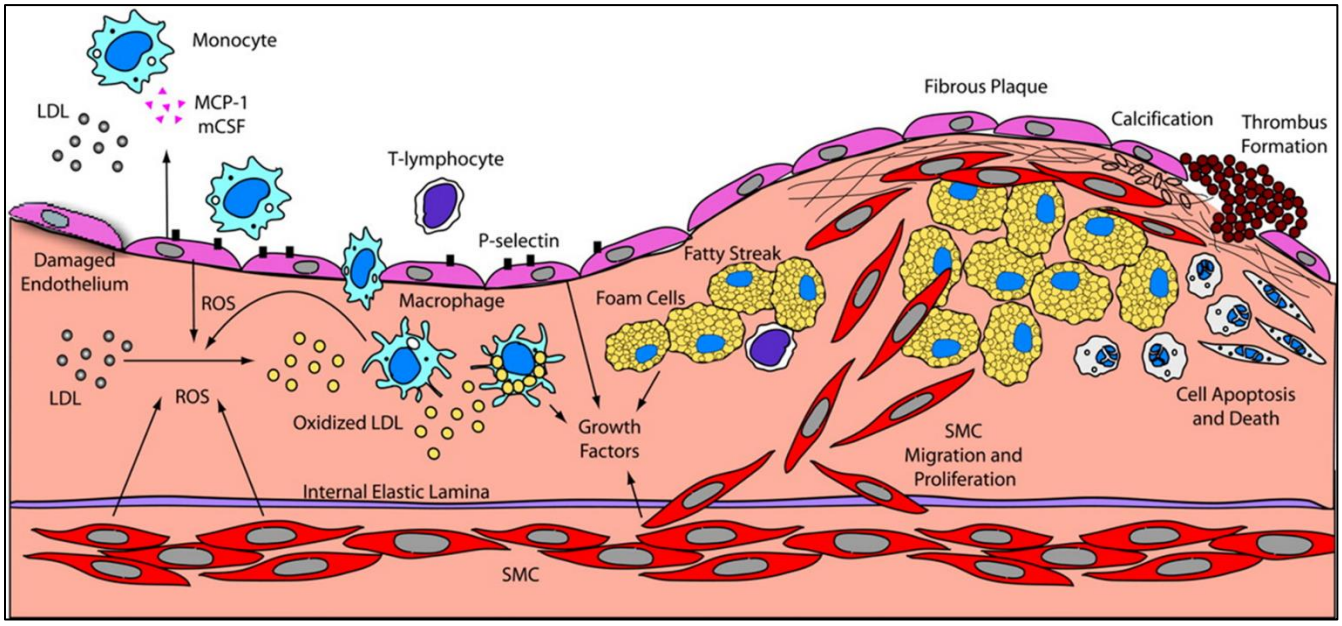

Figure 1: Development of an atherosclerotic lesion [3]**.** This process begins when LDL (so called bad cholesterol) enters the subendothelial space. LDL becomes oxidized to form oxLDL. Monocytes are recruited to the area and differentiate into macrophages in the subendothelial space. After the macrophages engulf the LDL, this causes an increase of intercellular cholesterol and this creates a foam cell. The foam cells and other immune cells release growth factors which recruit more macrophages, which become more foam cells. Vascular smooth muscle cells (VSMC) are recruited to the area and overlay the lesion. VSCM secrete ECM components to help stabilize the lesion. As the lesion progresses it may become calcified by mechanisms involving the trans-differentiation of VSMC into osteoblast-like cells. This creates a plaque. If a plaque becomes unstable and ruptures a thrombosis composed of platelets can form and break off and cause blockage leading to heart attacks and strokes. This figure was obtained from "Oxidative Stress and Vascular Disease" by Nageswara R. Madamanchi, Aleksandr Vendrov, and Marschall S. Runge. [3]

The calcification of vasculature is strongly correlated with the clinical manifestations of atherosclerosis. It is thought that calcification in arteries occurs in a process similar to skeletal bone remodeling and involves the osteogenic trans-differentiation of SMC within the walls of arteries that induces an active cell-mediated program that modulates deposition of bone matrix in blood vessels [5]. This process contains similar cells to osteoclasts (bone-destroying cells) and osteoblasts (bone-forming cells). Osteoblast-like cells are derived from trans-differentiated VSMC and are triggered by oxidative stress and the presence of phosphate [6]. Calcification occurs when the balance between osteoblasts and osteoclasts is not maintained, resulting in more calcium deposition than uptake. However, a complete understanding of the atherosclerotic calcification process is still unknown.

In calcified blood vessels, bone-related transcription factors including runt-related transcription factor 2 (RUNX2), and osterix (OSX) have been detected in populations of smooth muscle cells [5]. These transcription factors upregulate bone and chondrocyte proteins and control processes critical for osteoblast differentiation [5]. RUNX2 is required for early commitment of progenitor cells to differentiate into osteoblasts [7]. Osterix (OSX) is an osteoblast-specific transcription factor that acts downstream of RUNX2 [8]. Gene deletion studies have shown through the absence of RUNX2 or OSX, that these transcription factors are essential for osteoblast differentiation [9]. Osteoblasts are also an important marker in advanced atherosclerotic lesions. Osteoblastic activity can be detected by measuring calcium deposition, because osteoblasts are calcium-depositing cells. Osteopontin (OPN) is a protein that serves as a regulator for bone remodeling and is a potent inhibitor of vascular calcification [10].

OPN is expressed in the mineralized bone matrix, in macrophages, endothelial cells, smooth muscle cells and epithelial cells and serves as a marker of atherosclerotic calcification and indicates the presence of mature, calcium depositing osteoblasts [10]. Figure 2 below demonstrates the timeline of a progenitor cell transforming into a committed osteoblast, to a mature osteoblast and finally into an osteocyte. The figure also illustrates where in the process the markers (RUNX2, OSX and OPN) can be detected.

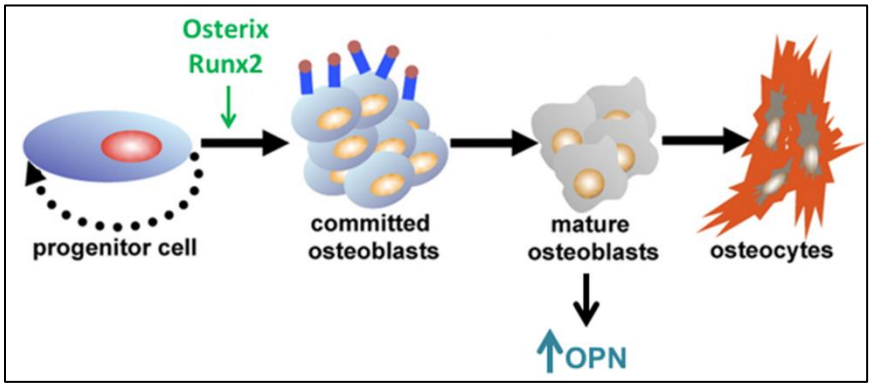

Figure 2: Timeline of a progenitor cell to an osteocyte and the position of the osteogenic markers in the process.

The Endocannabinoid System

Cannabinoids are molecules that are structurally similar to Δ^9 -tetrahydrocannabinol (THC), the primary psychoactive component in marijuana. Beginning from the known effects of smoking marijuana on heart rate and blood pressure, the cardiovascular effects of this compound were further investigated [11]. Since its discovery, the endocannabinoid system's role as a key signaling system has been found to take a part in nearly all physiological and pathological functions in mammals [11]. The endocannabinoid system has been shown to play a role in a wide

variety of processes including: memory, appetite, metabolism, stress and anxiety, analgesia, thermoregulation, sleep and immune cell function [12].

The endocannabinoid system comprises two distinct membrane G-protein-coupled receptors that have been identified by molecular cloning [13]. These two receptors, cannabinoid receptor type 1 (CB1) and cannabinoid receptor type 2 (CB2) and their endogenous ligands (called endocannabinoids) make up the endocannabinoid system. The CB1 receptor is primarily located in the central nervous system (brain and spinal cord) where it moderates the neurological and psychotropic effects of cannabinoids, but is also found in peripheral tissues and immune cells [13]. The CB2 receptor is predominantly expressed in peripheral immune cells [14]. It is believed that the immunomodulatory effects of cannabinoids are mediated by CB2 receptors expressed on immune cells [13]. Our lab has previously shown that mice lacking the CB2 receptor develop more calcification plaques compared to wild type mice with the CB2 receptor. However, both receptors have been identified outside of their primary locations – including in vascular smooth muscle cells [11].

In addition to the CB1 and CB2 receptors, the endogenous ligands that activate these receptors (known as endocannabinoids) are a key part of this system. Endocannabinoids, such as anandamide (N-arachidonoyl-ethanolamine, AEA) and 2-arachidonoylglycerol (2-AG), are biologically active fatty acids that have been shown to present a therapeutic target for the treatment of hypertension, a major risk factor for atherosclerosis [13]. AEA is a partial agonist at the CB1 receptor and is a weak partial agonist at CB2. 2-AG is considered a full agonist toward the CB2 receptor [12]. Both AEA and 2-AG are synthesized locally and on demand from membrane phospholipids

and are subject to rapid turnover, which limits their signaling to autocrine and paracrine mechanisms [12]. Both CB1 and CB2 have been shown to affect the formation of atherosclerotic lesions in studies of animal models [11] [15].

In contrast to the endogenous agonists, a known antagonist of these receptors is SR-144,528. A synthetic cannabinoid, SR-144,528, is characterized as a highly potent, selective and orally active antagonist for the CB2 receptor [16]. In an experimental mouse model of atherosclerosis, administration of low-dose THC resulted in the significant inhibition of plaque development, an effect that could be reversed by the co-administration of SR-144,528 [13].

As atherosclerosis was further understood as an inflammatory disease of the vasculature, studies investigating the possibility of an immunoregulatory effect of atherosclerosis by the endocannabinoid system have increased. In animal models, CB1 and CB2 have been shown to affect the formation of atherosclerotic lesions [11]. Generally, CB1 and CB2 have opposite effects. For example, CB1 activation often provides a pro-inflammatory and pro-atherosclerotic effect and activation of CB2 induces the opposite effect. Both receptors have also been implicated in having a role in the regulation of bone mass and bone remodeling through altering differentiation of precursor cells [17]. Mice lacking the CB2 receptor have been shown to have an accelerated age-related bone loss, which is similar to osteoporosis in humans [18]. As bone loss is inversely correlated with calcification in atherosclerotic lesions, these results further suggest that the CB2 receptor may play a role in the calcification process in atherosclerotic plaques.

Justification and Objective

We hypothesized that endocannabinoids modulate calcification of plaques by affecting osteogenic trans-differentiation of vascular smooth muscle cells (VSMC). Cannabinoid receptors are known to modulate bone formation and are present in elevated levels in atherosclerotic lesions and vessels, which lead us to suggest that they may also play a role in modulating calcification of these lesions. To begin to test this hypothesis, we evaluated the effects of two endocannabinoids (2-Arachidonoylglycerol and Anandamide) on the expression of osteogenic marker proteins by VSMC undergoing trans-differentiation to osteoblast-like cells.

Materials and Methods

Cell Culture

A transformed murine vascular smooth muscle cell line (MOVAS-1) was purchased from the American type culture collection (ATCC, VA, USA). MOVAS-1 cells were maintained in modified Dulbecco's Modified Eagle Medium (DMEM) (ATCC #30-2002) containing 4.5 g/L D-Glucose, 1.5 g/L sodium bicarbonate and supplemented with 10% fetal bovine serum, 0.2 mg/ml G-418, and 1% penicillin-streptomycin. The cells were maintained in a 5% CO_2 / 95% air humidified incubator.

Osteoblast Trans-differentiation

MOVAS-1 cells were seeded at 100,000 cells per plate in 35mm tissue culture dishes containing 2 mL of standard growth media. The media was replaced every other day until the cells reached a confluent monolayer in the dish, usually 24-48 hours after plating. Once confluent, the standard media was then replaced with osteogenic media (standard media supplemented with 2.6 mM Phosphate, pH 7.4). Controls were maintained in standard growth media. The cells were re-fed osteogenic media every two or three days as necessary. After 3-7 days of treatment, calcium deposition and expression of osteogenic marker proteins were evaluated by Alizarin Red staining and western blotting, respectively.

Treatment with Synthetic Cannabinoids

Once confluent, the cells were switched to osteogenic media supplemented with endocannabinoids. Supplements of 2-Arachidonylglycerol (2-AG) and/or anandamide (AEA) (Tocris Bioscience, Bristol, UK) and SR-144,528 (Biomol, Hamburg, DE) were

added to the osteogenic media. Treatments containing endocannabinoids (2AG, AEA) were present at 5 µM concentrations and treatments containing SR-144,528 were present in 2 µM concentrations. Controls received equal amounts of vehicle (DMSO). The media was replaced every 2-3 days as needed.

Preparation of Cell Lysates

The cells were washed twice with phosphate buffered saline (PBS) and collected in ice-cold 1X cell lysis buffer (Cell Signaling Technology, MA, USA) supplemented with Protease Inhibitor Cocktail (Thermo Scientific, MA, USA). The cells were kept at 4°C for 10 minutes and then centrifuged for 15 minutes at 12,000 x g at 4°C. The protein concentrations of the supernatants were determined by micro-BCA assay (Thermo Scientific, MA, USA) with BSA as the standard. The protein concentration was compared to the standard curve of known concentrations to determine the protein concentration of the samples. Cell lysates were stored at -80°C until use.

Western Blotting

Equal amounts (20 µg) of cell lysates were subjected to SDS-PAGE on 4-12% Bis-Tris NuPAGE gels (Life Technologies, CA, USA) and transferred to polyvinylidene fluoride membranes. The membranes were blocked in tris buffered saline containing 0.2% Tween-20 (TBS-T) and 5% nonfat dry milk for 1 hour followed by overnight incubation at 4°C in TBS-T containing a 1:1000 dilution of a primary antibody: Anti-RUNX2 (Santa Cruz Biotechnology, Dallas, TX), Anti-OPN (R30 Systems, Minneapolis MN), Anti-OSX (Aviva Systems Biology, San Diego, CA). The membranes were washed 5 times with TBS-T and then incubated for 1 hour with an HRP-conjugated secondary

antibody. After washing 5 times with TBS-T, the bands were visualized using an ECL Prime Western Blotting Detection Reagent (GE Healthcare, Pittsburg, PA) and a LAS-4000 image analyzer (GE Healthcare, Pittsburg, PA). To control for equal protein loading and transfer, the membranes were rinsed with TBS-T and subjected to the immunoblotting procedure using a 1:1000 dilution of a primary antibody to ß-actin (ProSci, San Diego, CA). Densitometry analysis of the relative band densities was performed using NIH ImageJ software. The results were normalized to ß-actin to correct for slight variations in protein loading and transfer efficiency.

Alizarin Red Staining

Alizarin Red staining was performed to stain the cell matrix monolayer for calcium deposits. The media was aspirated from the plates and phosphate buffered saline (PBS) was used to wash the cells twice. The cells were then fixed with 10% buffered formalin for 10 minutes and subsequently rinsed with PBS. The cells were then stained with a 2% Alizarin Red solution (Electron Microscopy Sciences, Hatfield, PA) for 30 minutes, followed by three 1-minute rinses with distilled water. After staining, the cells were digitally photographed.

Quantitation of Alizarin Red Staining

After digital photography of the Alizarin Red stained cells, the bound Alizarin Red was extracted from the cells by incubating in 2 mL of 10% cetylpyridinium chloride. The absorbance at 562 nm was then measured using a microplate reading spectrophotometer to quantify the amount of extracted dye from each plate.

Image Analysis using ImageJ Software

Quantification of the resultant bands from the Western blots and analysis of the degree of alizarin Red staining in digital images was performed using computer-assisted morphometric analysis software (ImageJ, NIH). For quantification of Alizarin Red staining, 4X photomicrographs were obtained using a light microscope equipped with a charge coupled device (CCD) camera attached to a PC. Photomicrographs (4X) were taken at 3 random microscopic fields and analyzed using ImageJ by thresholding for the red pixel color. The thresholding parameters were held constant for all images examined and the results were expressed as the area of the image occupied by red divided by the total area of the image. To quantify the Western blot bands, digital images of the blots were evaluated using the standard procedure from NIH. The optical density recorded for each band was normalized to the optical density of the corresponding band for ß-actin. The ratio obtained for the standard media sample was set as 1.0 and used to calculate the fold difference. The data was then presented as the mean ± S.D. of three replicate western blots.

Statistical Analysis

Student t-tests were performed using SPSS Version 12.0 statistic software package. P-values < 0.05 were considered statistically significant.

Results

To begin to access the potential effect of endocannabinoid supplementation on osteogenic trans-differentiation of vascular smooth muscle cells, MOVAS-1 cells were cultured in osteogenic media (2.6 mM P_i) containing 2-Arachidonylglycerol (2-AG), anandamide (AEA), 2-AG and AEA together, or 2-AG, AEA and SR-144,528, a CB2 selective antagonist. After 3 and 5 days of treatment, the MOVAS-1 cells were stained with Alizarin Red to access the degree of calcium deposition (Figures 3 and 4). The trends seen in Figure 3 and 4 demonstrate that calcification is a time dependent process – with photographs taken at 5 days exhibiting a higher degree of positive staining than the photos taken at 3 days. Supplementation with 2-AG or AEA alone, and in combination, resulted in visibly more calcium deposition compared to the cells cultured in osteogenic media alone. However, co-treatment with SR-144,528 did not appear to alter the degree of calcium deposition in response to 2-AG and AEA.

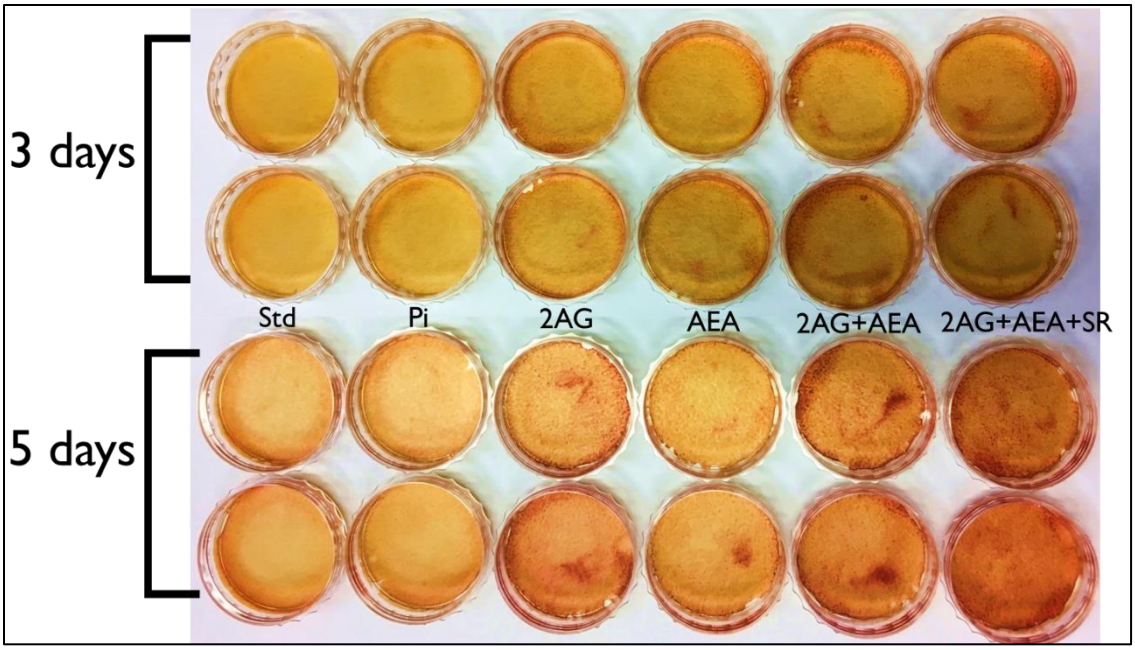

Figure 3: MOVAS-1 cells stained with Alizarin Red. After treatment, the MOVAS-1 cells were stained with Alizarin Red. The treatment groups are listed horizontally indicating standard growth media (Std), osteogenic media (2.6 mM Pi), 5 µM 2-AG alone (2AG), 5 µM AEA alone (AEA), 5 µM of both endocannabinoids in combination (2AG+AEA), as well as the combination of 5 µM of 2-AG and AEA with the addition of 2 µM SR-144,528 (2AG+AEA+SR). The top panel shows results of cells treated for 3 days. The bottom panel shows results of cells treated for 5 days.

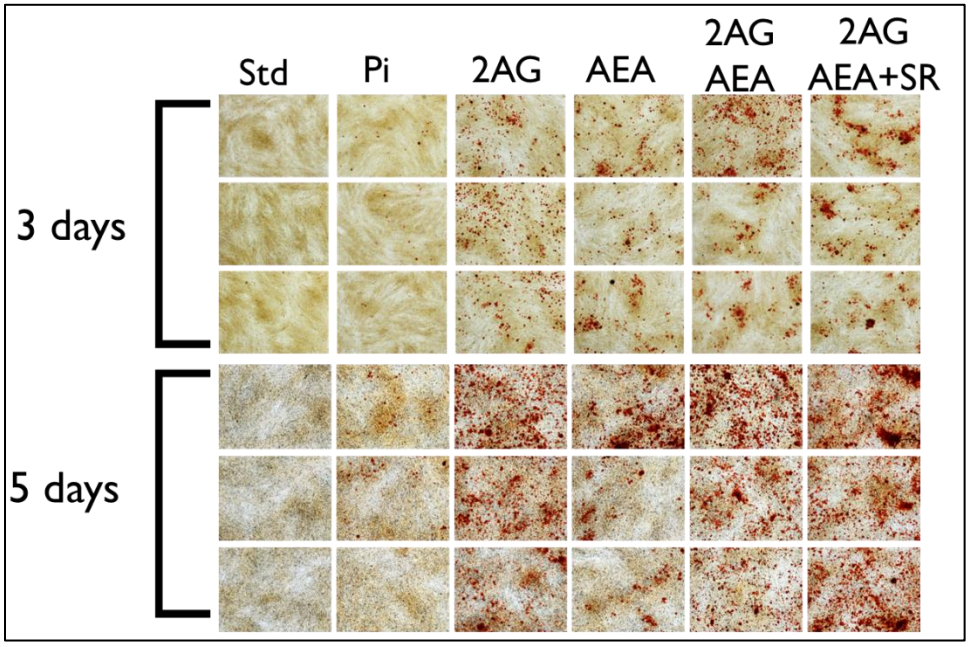

Figure 4: Photomicrographs of Alizarin Red stained MOVAS-1 cells. Corresponding to the same Alizarin Red stained plates from Figure 3, three random microscopic fields were photographed at 4X magnification. The top panel indicates staining results from the 3-day treatment group. The bottom panel demonstrates results from the 5-day treatment group.

To quantify the degree of Alizarin Red staining present in the figures above, two methods were employed. First, the amount of Alizarin Red stain bound to the plate was evaluated by computer assisted morphometric analysis of digital photomicrographs to measure the percent of the total area stained by Alizarin Red. The results, presented in Figure 5, revealed that supplementation with 2-AG or AEA alone produced a statistically significant ($p < 0.05$) increase in calcium deposition at 3 days when compared to the corresponding osteogenic media only treatment, but only the 2-AG group was significantly greater after 5 days. Treatment with both AEA and 2-AG also resulted in a statistically significant increase in calcium deposition after 5 days. However, co-treatment with SR-144,528 did not have a statistically significant effect on induction of calcium deposition by 2-AG and AEA.

A second method was utilized to verify the results of the digital quantitation of the Alizarin Red staining. The bound Alizarin Red was extracted with 10% cetylpyridinium chloride and the absorbance of the Alizarin Red dye extracted from each plate was measured spectrophotometrically at 562 nm (Figure 6). The results obtained with this method are in general agreement with those for the digital quantification methods shown in Figure 5. However, both 2-AG and AEA alone as well as in combination produced statistically significant results at 3 and 5 days. The results also indicated that the when the endocannabinoid combination (2-AG+AEA) was compared to the combination with SR-144,528 added, the results were not statistically significant ($p < 0.05$).

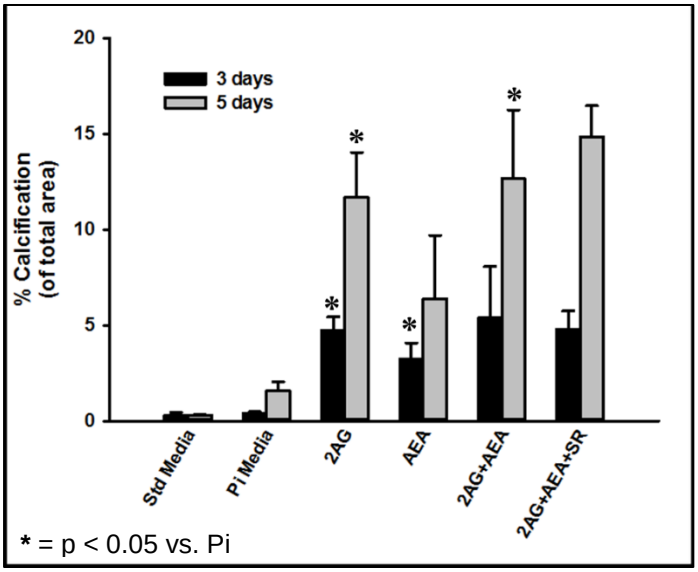

Figure 5: Quantitation of calcium deposition detected by Alizarin Red staining using computer assisted morphometric analysis. The area occupied by red pixels present in three random photomicrographs shown in Figure 3 was obtained by thresholding for the area occupied by red and dividing by the total area of the digital image. The results are presented as the mean percent calcification ± the standard deviation (SD) of three random fields. Asterisks (*) indicate $p < 0.05$ compared to cultured osteogenic media (Pi) alone.

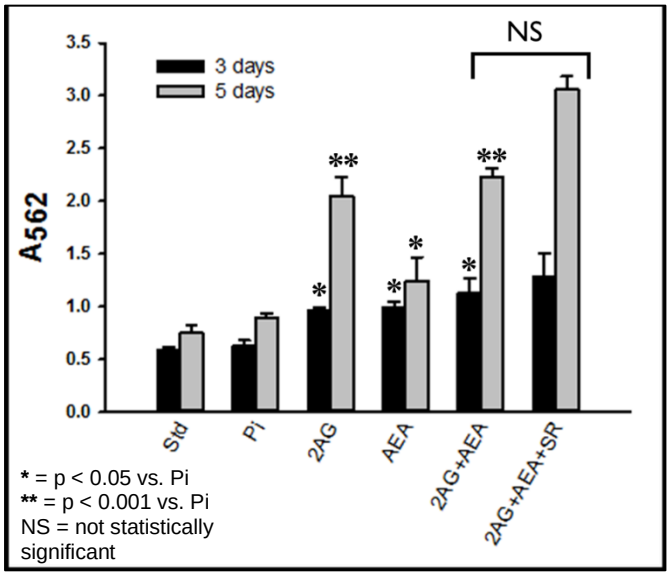

Figure 6: Quantitation of calcium deposition by extraction of Alizarin Red with cetylpyridinium chloride. Alizarin Red bound to each plate was extracted using 10% cetylpyridinium chloride and the absorbance was determined spectrophotometrically at 562 nm. The results are presented as the mean ± the standard deviation (SD) of three replicate treatments. Asterisks (*) indicates $p < 0.05$ and (**) indicates $p < 0.001$ compared to cultured osteogenic media (Pi) alone.

Three osteogenic marker proteins were examined to investigate the effects of endocannabinoid treatment on the osteogenic trans-differentiation of the MOVAS-1 cells at the molecular level. These markers include Runt related transcription factor 2 (RUNX2), Osteopontin (OPN), and Osterix (OSX). From the western blots (Figure 7) and subsequent graphs (Figures 8-10), it can be observed that expression of OSX and RUNX2 varied only slightly with the addition of endocannabinoids and with addition of a CB2 inhibitor. However, OPN levels were strikingly induced by the addition of 2-AG and AEA alone and more so when used in combination. The induction of OPN expression was greatly reduced by co-treatment with SR-144,528, indicating a CB2-dependent effect by 2-AG/AEA on expression of OPN. In contrast, co-treatment with SR-144,528 had little or no effect on the expression levels of OSX and RUNX2.

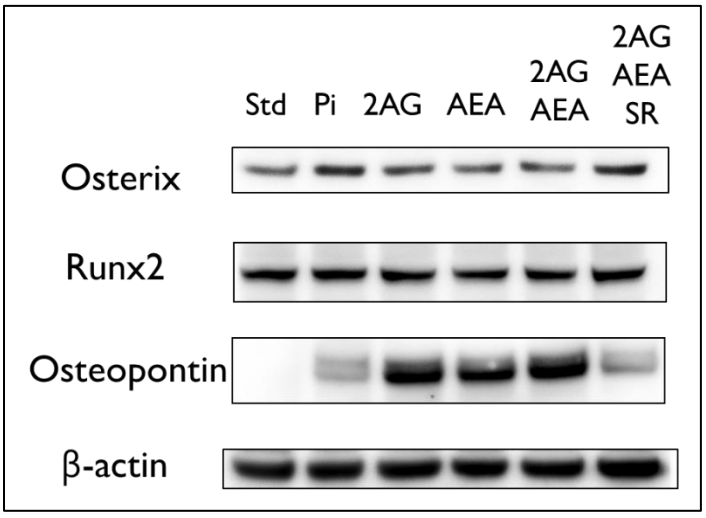

Figure 7: Expression of osteogenic marker proteins in MOVAS-1 cells. Following 7 days of endocannabinoid treatment, cell lysates were prepared and analyzed by western blotting to compare the expression levels of OSX, RUNX2, and OPN. Beta actin expression was also evaluated as a loading control. The labels at the top of the figure correspond to standard growth media (Std), osteogenic media (2.6 mM Pi), 5 µM 2-AG, 5 µM AEA, 5 µM of both 2-AG and AEA in combination (2AG+AEA), and the 5 µM combinations with the addition of 2 µM SR-144,528 (2AG+AEA+SR). Results shown are representative of three western blotting experiments.

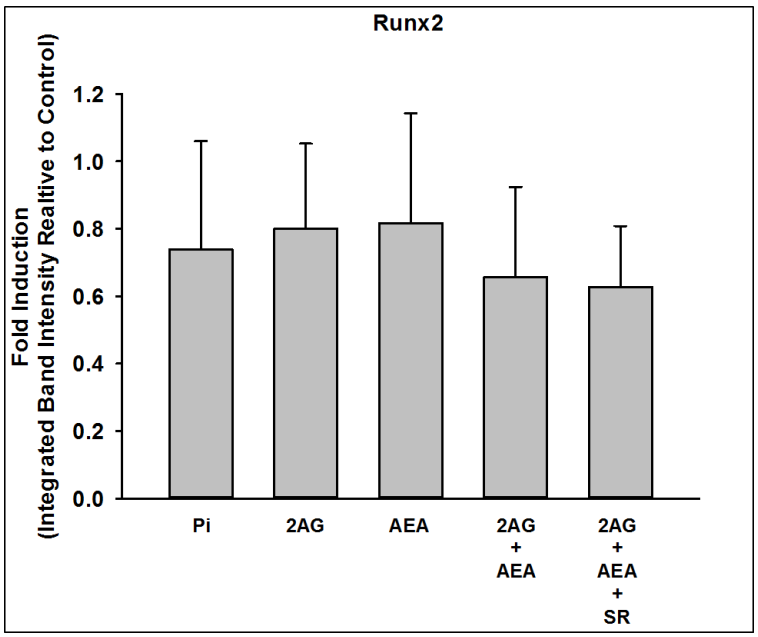

Figure 8: RUNX2 expression levels following 7 days of endocannabinoid treatment. The ratio of RUNX2 to ß-actin was determined by quantifying the relative band densities and compared to the value determined for MOVAS-1 cells cultured in standard media alone to give the fold induction. The results are presented as the mean ± the standard deviation of three western blot experiments.

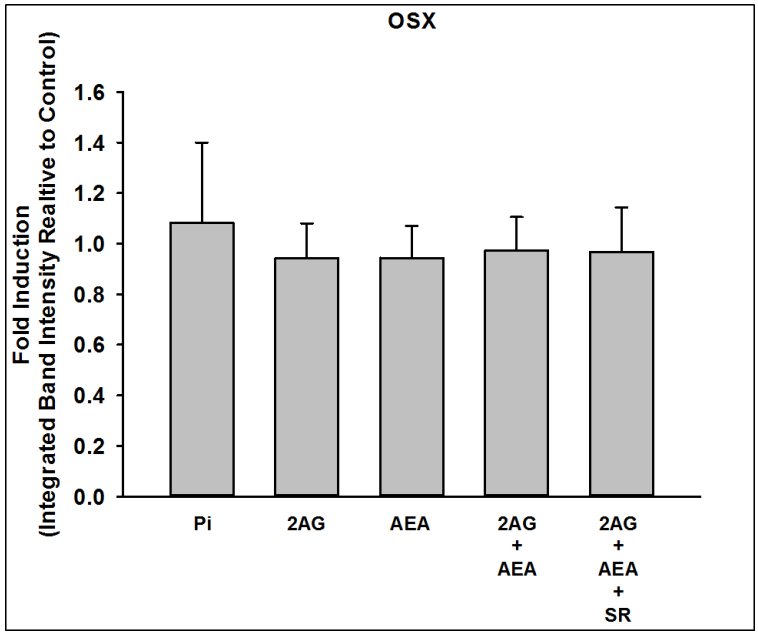

Figure 9: OSX expression levels following 7 days of endocannabinoid treatment. The ratio of OSX to ß-actin was determined by quantifying the relative band densities essentially as described for Figure 8. The results are presented as the mean ± the standard deviation of three western blot experiments.

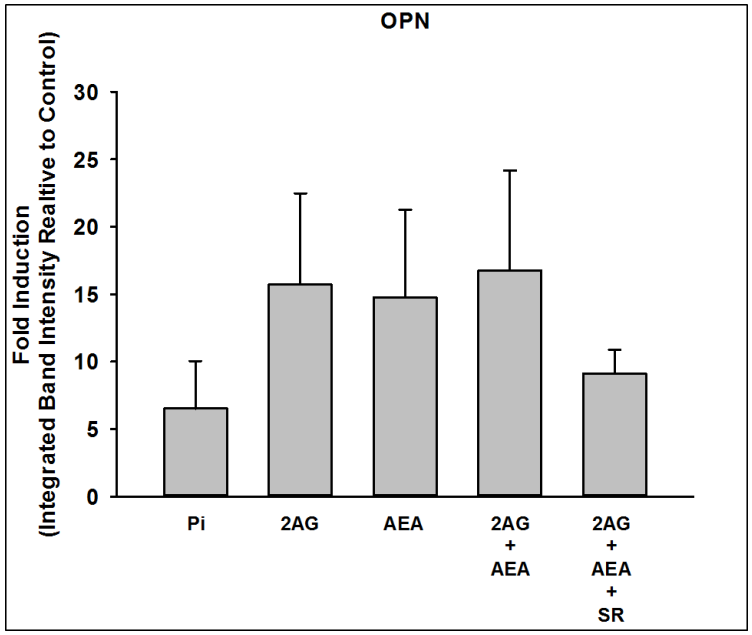

Figure 10: OPN expression levels following 7 days of endocannabinoid treatment. The ratio of OPN to ß-actin was determined by quantifying the relative band densities essentially as described for Figure 8. The results are presented as the mean ± the standard deviation of three western blot experiments.

Discussion

Currently, atherosclerosis is the leading cause of death in the United States. The current treatment options primarily target only the risk factors for atherosclerosis – such as aiming to inhibit high cholesterol levels, diabetes mellitus, obesity, and hypertension. The calcification seen in advanced atherosclerotic lesions is strongly correlated with increased risk for myocardial infarction (heart attacks) and strokes. There is no known cure for atherosclerosis, the best therapies merely help slow the formation of plaques but cannot prevent their formation or calcification. This is largely because the mechanisms controlling atherosclerotic calcification are unknown. It has been demonstrated that cannabinoid receptors modulate bone formation and are present in high concentrations in atherosclerotic vessels, suggesting they may also play a role in modulating calcification. Therefore, we tested the hypothesis that endocannabinoids modulate calcification of plaques by affecting osteogenic trans-differentiation of vascular smooth muscle cells (VSMC). We evaluated the effects of the two best-described endocannabinoids (2-Arachidonoylglycerol, Anandamide) on the osteoblastic trans-differentiation of MOVAS-1 cells undergoing calcification to determine their role in the calcification process. The MOVAS-1 cell line, a murine VSMC model was chosen as the model because of its ability to differentiate spontaneously into osteoblast-like cells when cultured in an osteogenic media [19].

It was observed that calcification, as detected by Alizarin Red staining, increased in a time dependent manner in osteogenic media (Figures 3-6). Quantitation of the Alizarin Red staining revealed that the addition of endocannabinoids to the osteogenic media increased the amount of calcification (Figure 5 and 6). A significant increase was

noted with the addition of endocannabinoids when compared to the control group (Figure 6). However, the addition of SR-144,528, a CB2 selective inhibitor, did not have a significant effect on the degree of calcification present in the MOVAS-1 cells. These results indicate that endocannabinoids (2AG, AEA) accelerate MOVAS-1 calcification by a mechanism that is independent of CB2 activity. As MOVAS-1 cells also express CB1, it is possible that this alternative mechanism stems through the activation of the CB1 receptor, or perhaps, via another uncharacterized endocannabinoid receptor. Alternatively, 2-AG/AEA may induce calcium deposition by a mechanism that is independent of a cell surface receptor. Further investigation is necessary to better understand how endocannabinoids alter calcium deposition in MOVAS-1 cells.

Three osteogenic marker proteins were examined to further investigate the effects of endocannabinoids on the osteogenic trans-differentiation of the MOVAS-1 cells. Expression of both RUNX2 and Osterix (OSX) were both minimally affected by the endocannabinoid treatments and were not affected by the inclusion of a CB2 antagonist. This result suggests a CB2-independent effect of 2AG and AEA on the levels of RUNX2 and OSX during MOVAS-1 calcification. Further studies to test the effects on RUNX2 and OSX activity are needed to better determine how endocannabinoids modulate trans-differentiation of MOVAS-1 cells. Interestingly, a CB2-dependent effect was observed on osteopontin levels. This was evident with the increase in OPN expression seen with the addition of endocannabinoids and the dramatic reduction in this effect upon co-treatment with a CB2 antagonist. Future investigation should help establish the degree by which CB2 signaling modulates expression of OPN in MOVAS-1 cells and other VSMCs.

In conclusion, the work in this thesis demonstrates a potential role for endocannabinoids in moderating the lesion calcification process in atherosclerosis by altering VSMC trans-differentiation. This study also highlights the need for further research to investigate the CB1 and CB2 dependent effects of this process on the development of advanced atherosclerotic lesions. Confirmation of a role for CB2 in atherosclerotic lesion calcification would be a potentially major clarification of the little-understood phenomenon of advanced lesion calcification. This thesis embodies the beginning phases of the development of an in-vitro model of the complex signaling mechanisms involved in the endocannabinoid effect on controlling the differentiation of VSMC. Ultimately, investigations in animal models of atherosclerosis could be designed to test potential novel mechanisms so that the formation and calcification of atherosclerotic plaques may be prevented or reversed. If successful, these therapies could be applied to clinical studies targeting atherosclerotic vessels in patients and ultimately provide some alleviation of the strain that cardiovascular diseases currently place on our society.

Acknowledgments

This work was supported by grants obtained through the National Institutes of Health grant (R15HL113878 and C06RR0306551). I would like to personally thank Dr. Douglas Thewke for his immense assistance, support, and instruction during the completion of my research and thesis writing. I would also like to thank Makenzie Fulmer for her mentorship and assistance in the laboratory. A special thank you to my readers, Dr. Kornweibel and Dr. Rusiñol for taking the time to read and help me finalize my thesis. I would also like to acknowledge East Tennessee State University Honors College, specifically the Midway Honors Scholars program and the Honors-In-Discipline Chemistry Program, for providing me the education and opportunity to take part in undergraduate research. Finally, I would like to thank various friends and family members for the support throughout my college endeavors.

References

[1] C. H. Byon, "Runx2-Upregulated Receptor Activator of Nuclear Factor κB Ligand in Calcifying Smooth Muscle Cells Promotes Migration and Osteoclastic Differentiation of Macrophages," *Arteriosclerosis, Thrombosis, and Vascular Biology,* vol. 31, no. 6, pp. 1387-1396, 2011.

[2] J. F. Bentzon, "Mechanisms of Plaque Formation and Rupture," *Circulation Research,* vol. 114, no. 12, pp. 1852-1866, June 2014.

[3] N. R. Madamanchi, "Oxidative Stress and Vascular Disease," *Arteriosclerosis, Thrombosis, and Vascular Biology,* vol. 25, no. 1, pp. 29-38, 2005.

[4] M. J. Budoff, "Thoracic Aortic Calcification and Coronary Heart Disease Events: the Multi-Ethnic Study of Atherosclerosis (MESA)," pp. 196-202, 2011.

[5] J. A. Leopold, "Vascular calcification: Mechanisms of vascular smooth muscle cell calcification," *Trends in Cardiovascular Medicine,* vol. 25, no. 4, pp. 267-274, 2015.

[6] B. Thompson, "Arterial calcification and bone physiology: role of the bonevascular axis," *Nat Rev Endocrinol,* vol. 8, no. 9, pp. 529-543, 2012.

[7] T. Tanaka, "Runx2 Represses Myocardin-Mediated Differentiation and Facilitates Osteogenic Conversion of Vascular Smooth Muscle Cells," *Molecular and Cellular Biology,* vol. 28, no. 3, pp. 1147-1160, 2008.

[8] A. Alexopoulosa, "Bone regulatory factors NFATc1 and Osterix in human calcific aortic valves," *International Journal of Cardiology,* vol. 139, no. 2, pp. 142-149, 2010.

[9] D. J. Hadjidakis, "Bone Remodeling," *Annals of the New York Academy of Science,* vol. 1092, pp. 385-396, 2006.

[10] T. Wolak, "Osteopontin – A multi-modal marker and mediator in atherosclerotic vascular disease," *Atherosclerosis,* vol. 236, no. 2, pp. 327-337, 2014.

[11] F. Montecucco, "At the heart of the matter: the endocannabinoid system in cardiovascular function and dysfunction," *Trends in Pharmacological Science,* vol. 33, no. 6, pp. 331-340, 2012.

[12] A. M. Malfitano, "What We Know and Don’t Know About the Cannabinoid Receptor 2 (CB2)," *Seminars in Immunology,* vol. 26, pp. 369-379, 2015.

[13] F. Mach, "The Role of the Endocannabinoid System in Atherosclerosis," *The Journal of Neuroendocrinology,* vol. 20, no. s1, pp. 53-57, 2008.

[14] S. Singla, "Cannabinoids and Atherosclerotic Coronary Heart Disease," *Clinical Cardiology,* vol. 35, no. 6, pp. 329-335, 2012.

[15] D. Thewke, "Cannabinoid Receptor Type 2 (CB2) Dependent and Independent Effects of WIN55,212-2 on Atherosclerosis in Ldlr-null Mice," *Journal of Cardiology and Therapeutics,* vol. 3, no. 2, 2015.

[16] M. Rinaldi-Carmona, "SR 144528, the First Potent and Selective Antagonist of the CB2 Cannabinoid Receptor," *Journal of Pharmacology and Experimental Therapeutics,* vol. 284, no. 2, pp. 644-650, 1998.

[17] T. J, "Involvement of Neuronal Cannabinoid Receptor CB1 in Regulation of Bone Mass and Bone Remodeling," *Molecular Pharmacology,* vol. 70, no. 3, pp. 786-792, 2006.

[18] A. Zimmer, "Endocannabinoids and the Regulation of Bone Metabolism," vol. 20, no. S1, pp. 69-74, 2008.

[19] "MOVAS-1 cell line: A new in vitro model of vascular calcification," *International Journal of Molecular Medicine,* vol. 27, no. 5, 2011.